Crystal Structure and Spectroscopic Characterization of $CsV(SO_4)_2$. Evidence for an Electronic Raman Transition

R. W. Berg,*[1a] S. Boghosian,[1b] N. J. Bjerrum,[1a] R. Fehrmann,[1a] B. Krebs,[1c] N. Sträter,[1c] O. S. Mortensen,[1d] and G. N. Papatheodorou[1b]

Institute of Inorganic Chemistry, University of Münster, D-48149 Münster, Germany, and Chemistry Department A, Technical University of Denmark, DK-2800 Lyngby, Denmark

Received December 23, 1992®

Green platelike hexagonal crystals of $CsV(SO_4)_2$ were obtained by stepwise cooling in the range 500–400 °C of solutions of V_2O_5 in $Cs_2S_2O_7$, either under SO_2(g) atmosphere or during catalytic conversion of SO_2, in a 10% SO_2, 11% O_2, and 79% N_2 gas mixture. The crystals belong to the trigonal system, space group $P\bar{3}$, with $a = b = 4.868(1)$ Å and $c = 8.767(2)$ Å at 140 K and $Z = 1$. The phase represents a novel structure type with tetrahedral SO_4^{2-} ions linked to octahedrally coordinated vanadium(III) in a way different from the known $KV(SO_4)_2$ and other related $M^IM^{III}(SO_4)_2$ structures. The infrared and Raman spectra of powdered $CsV(SO_4)_2$ show close analogy to those of $KV(SO_4)_2$. The crystal Raman spectra show vibrational bands the polarization properties of which cannot be explained in terms of the crystallographic point group and a totally symmetric electronic ground state. Above 1300 cm^{-1} the Raman spectra, particularly at lower temperatures, show a coarse structure, which is interpreted as electronic Raman transitions between the spin–orbit split states of the ^3A_g and ^3E_g levels.

Introduction

The molten salt-gas system $M_2S_2O_7/V_2O_5$-$SO_2/O_2/SO_3/N_2$ (M = Na, K, Cs) at 400–600 °C is a realistic model of the working industrial catalyst utilized for the production of sulfuric acid, i.e. catalyzing the reaction $SO_2 + {}^1/_2O_2 \rightleftharpoons SO_3$. The catalyst is usually promoted by K and minor amounts of Na. At lower temperatures, i.e. below 440 °C, the activity of the commercial catalysts decreases sharply[2] due to the precipitation of V(IV) and V(III) compounds.[3,4] These compounds have been identified as $KV(SO_4)_2$, $K_4(VO)_3(SO_4)_5$, $NaV(SO_4)_2$, and $Na_2VO(SO_4)_2$, and we have published their crystal structures and vibrational spectra.[5–8] Catalysts promoted by Cs or Rb have a higher activity in the low-temperature region and commercial catalysts containing Cs (besides K and Na) have been developed. Recently,[9,10] we have investigated the binary system, $Cs_2S_2O_7$–V_2O_5, which is a model of the oxidized form of a pure Cs promoted catalyst with vanadium present in the +5 oxidation state only. During deactivation of the Cs-based catalyst in the presence of SO_2(g), the blue V(IV) compound, $Cs_2(VO)_2(SO_4)_3$ and the green V(III) compound $CsV(SO_4)_2$ are formed.[3] The crystal structure and vibrational spectra of the former compound will be the object of a future publication,[11] whereas this investigations is concerned with the latter compound, $CsV(SO_4)_2$.

Experimental Section

The equipment has been described in detail.[3,6] It includes a gas mixing unit equipped with mass flowmeters and a gas preconverter whereby any desired $SO_2/O_2/SO_3/N_2$ gas mixture can be obtained. Ampoules were heated in a quartz tube furnace controlled to ±2 K with a chromel–alumel thermocouple.

Materials. $Cs_2S_2O_7$ was obtained by thermal decomposition of $Cs_2S_2O_8$. These salts are not commercially available. The synthesis of $Cs_2S_2O_8$ and $Cs_2S_2O_7$ has been described recently.[9] The purity of the $Cs_2S_2O_7$ (mp 461 °C) was checked by Raman spectroscopy as earlier described.[3] V_2O_5 was from CERAC (Pure, 99.9%). All handling of chemicals took place in a glovebox with a controlled water content not exceeding 5 ppm. The hygroscopic $Cs_2S_2O_7$ was stored in sealed glass ampules until used.

Synthesis of Crystalline $CsV(SO_4)_2$. The compound was obtained from molten mixtures of V_2O_5 and $Cs_2S_2O_7$ with molar ratios Cs/V = 3–10, contained in a reactor flow cell, as earlier described,[3] or in a sealed ampoule under 1 atm of SO_2(g). The chemicals were added to cells in the glovebox. During the interaction of a 10% SO_2, 11% O_2, and 79% N_2 gas mixture (by volume) with the melts, blue and green precipitates were formed when the temperature was gradually reduced from around 500 °C to a temperature in the range 430–388 °C. The design of the reactor cell permitted isolation of the formed crystals (by filtering on a sintered frit by reversing the gas flow), thus simulating practical catalytic conditions. In ampules with a melt composition of Cs/V = 4.8, precipitation was observed by lowering the temperature from 500 to 460 °C. A further decrease to 444 °C resulted in a large crop of mainly green hexagonal crystals, but also a small amount of blue crystals were observed. Generally blue crystals predominated the precipitates at low Cs/V ratios whereas the green compound was predominating at higher ratios. After cooling, the residual melt was dissolved in water, leaving the sparingly soluble blue and green crystals undissolved. The blue compound was found[3,11] to be the V(IV) salt $Cs_2(VO)_2(SO_4)_3$, whereas the green hexagonal crystals were the V(III) compound, $CsV(SO_4)_2$.

Infrared Spectra. IR spectra were recorded on a Bomem DA3.26 FTIR spectrometer. The samples were ground in dry CsBr and pressed into transparant disks.

Raman Spectra. Raman spectra were recorded on a JEOL JRS-400D spectrometer equipped with a double monochromator and a cooled S-20 photomultiplier calibrated to ±1 cm^{-1} with argon plasma lines. Some samples were contained in sealed glass tubes that could be immersed in liquid nitrogen in order to obtain spectra at 77 K.

Absorption Spectra. Absorption spectra were obtained on a Perkin-Elmer λ-9 spectrophotometer. The sample consisted of a cluster of large hexagonal platelike crystals mounted on a copper foil with a convenient slit.

® Abstract published in *Advance ACS Abstracts*, September 15, 1993.

(1) (a) Technical University of Denmark. (b) Institute of Chemical Engineering and High Temperature Chemical Processes, University of Patras, P.O. Box 1414, GR-26500 Patras, Greece. (c) University of Münster. (d) Department of Physics, University of Odense, DK-5230 Odense M, Denmark.
(2) Villadsen, J.; Livbjerg, H. *Catal. Rev.—Sci. Eng.* **1978**, *17*, 203.
(3) Boghosian, S.; Fehrmann, R.; Bjerrum, N. J.; Papatheodorou, G. N. *J. Catal.* **1989**, *119*, 121.
(4) Eriksen, K. M.; Fehrmann, R.; Bjerrum, N. J. *J. Catal.* **1991**, *132*, 263.
(5) Fehrmann, R.; Krebs, B.; Papatheodorou, G. N.; Berg, R. W.; Bjerrum, N. J. *Inorg. Chem.* **1986**, *25*, 1571.
(6) Fehrmann, R.; Boghosian, S.; Papatheodorou, G. N.; Nielsen, K.; Berg, R. W.; Bjerrum, N. J. *Inorg. Chem.* **1989**, *28*, 1847.
(7) Fehrmann, R.; Boghosian, S.; Papatheodorou, G. N.; Nielsen, K.; Berg, R. W.; Bjerrum, N. J. *Acta Chem. Scand.* **1991**, *45*, 961.
(8) Fehrmann, R.; Boghosian, S.; Papatheodorou, G. N.; Nielsen, K.; Berg, R. W.; Bjerrum, N. J. *Inorg. Chem.* **1990**, *29*, 3294.
(9) Folkmann, G. E.; Hatem, G.; Fehrmann, R.; Gaune-Escard, M.; Bjerrum, N. J. *Inorg. Chem.* **1991**, *30*, 4057.
(10) Folkmann, G. E.; Hatem, G.; Fehrmann, R.; Gaune-Escard, M.; Bjerrum, N. J. *Inorg. Chem.* **1993**, *32*, 1559.
(11) Boghosian, S. *et al.* Work in progress.

0020-1669/93/1332-4714$04.00/0

Table I. Crystal Data, Data Collection, and Refinement of the Structure at 140 K for $CsV(SO_4)_2$

fw	375.974 g/mol
cryst size, mm^3	0.15 × 0.13 × 0.07
cryst syst	trigonal
space group	$P\bar{3}$ (No. 147)
unit cell	
a, Å	4.868(1)
c, Å	8.767(2)
V, $Å^3$	179.9
Z	1
D_{calc}, g cm^{-3}	3.471
D_{measd}, g cm^{-3}	3.44(4)
radiation	Mo Kα (λ = 0.710 69 Å)
monochromator	graphite (horizontal)
scan mode	2θ–θ
scan range in 2θ, deg	4–75
scan speed in 2θ, deg min^{-1}	3.0–29.3
abs coeff, mm^{-1}	6.85
min, max, transm	0.316, 0.685
no. of reflcns measd.	1350 ($+h,\pm k,\pm l$)
no. of reflcns after averaging	654
merging R factor	0.021
no. of reflcns for refinement	621 ($I > 2\sigma(I)$)
structure solution	Cs position by Patterson method; other atoms by difference-Fourier calc
refinement	all atoms with anisotropic temp factors
isotropic extinction param x[14]	0.013
$F^* = F_c/((1 + 0.002xF^2_c/(\sin 2\theta))^{0.25})$	
no. of variables	20
$R = \sum\|\|F_o\| - \|F_c\|\|/\sum\|F_o\|$	0.0213
$R_w = [\sum w(\|F_o\| - \|F_c\|)^2/\sum w\|F_o\|^2]^{1/2}$	0.0290
$w = 1/(\sigma^2(F_o) + 0.0001F_o^2)$	

X-ray Investigations

A green powder sample of $CsV(SO_4)_2$ has earlier[12] been prepared by drying redviolet $CsV(SO_4)_2 \cdot 12H_2O$ at 250 °C. The X-ray powder diffraction pattern of $CsV(SO_4)_2$ at room temperature has been published,[13] and the pattern was indexed in a hexagonal cell with $a = 4.88$ Å and $c = 9.04$ Å.

Determination of the Crystal Structure by Single-Crystal X-ray Diffraction Analysis. Intensity data were collected on a Syntex $P2_1$ single-crystal diffractometer at 140 K, using as a sample a light-green hexagonal, platelike crystal cooled in a nitrogen gas stream. High-precision unit cell dimensions were refined from high-angle reflection coordinates determined on the four-circle diffractometer. The single-crystal data and pertinent details on data collection and refinement of the structure are given in Table I. No phase transition was observed between 140 and 300 K.

Structure solution and refinement was done with the program system SHELXTL PLUS using scattering factors as tabulated in ref 15. A numerical correction for absorption was applied by indexing the well-defined faces of the platelike hexagonal crystal. The structure was refined using full matrix least-squares calculations as described by Cruickshank.[16] Though the weighted reciprocal lattice and the systematic absences indicated space group $P\bar{3}$ (of Laue symmetry $\bar{3}$) rather than $P321$ or $P\bar{3}m1$ (of Laue symmetry $\bar{3}m$), the structure was also refined in the space group $P321$, because many M^IM^{III} double sulfates are known to crystallize in this space group ($KAl(SO_4)_2$ type). However, the refinement in $P321$ presented serious correlation problems for oxygen coordinates and thermal parameters and resulted in a clearly worse R factor of 6.4% (same number of refined parameters). Consequently, the finding of $P\bar{3}$ as the correct space group is highly significant.

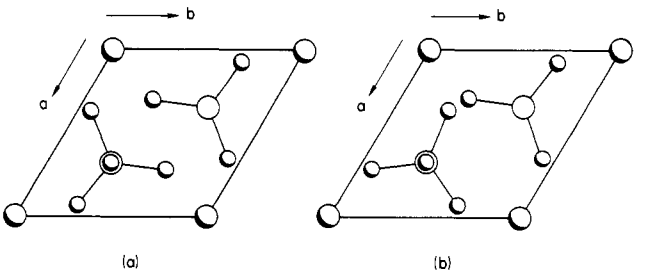

Figure 1. Projection of the $CsV(SO_4)_2$ structure in space group $P\bar{3}$ (a) as compared to the scaled $KAl(SO_4))_2$ structure in space group $P321$ (b).

Table II. Coordinates and Isotropic Temperature Factors of the Atoms for $CsV(SO_4)_2$ at 140 K (with Standard Deviations)

atom	site (multiplicity, symmetry)	x/a	y/b	z/c	U_{eq}[a]
Cs	a (1, $\bar{3}$)	0.0	0.0	0.0	0.0096(1)
V	b (1, $\bar{3}$)	0.0	0.0	0.5	0.0043(1)
S	d (2, 3)	0.66667	0.33333	0.6914(1)	0.0048(1)
O(1)	d (2, 3)	0.66667	0.33333	0.8566(2)	0.0097(4)
O(2)	g (6, 1)	0.3607 (3)	0.0704(3)	0.6340(1)	0.0075(3)

[a] U_{eq} was calculated as one third the trace of the orthogonalized U_{ij} matrix.

Figure 1 shows a projection of the $CsV(SO_4)_2$ structure in $P\bar{3}$ (a) and a scaled structure of the $KAl(SO_4)_2$ type in P321 (b). The two structures differ only in three of the six positions of atom O(2). This accounts for the remarkably low R factor of $CsV(SO_4)_2$ in the wrong space group $P321$.

Most of the compounds reported to crystallize in the $KAl(SO_4)_2$ structure type ($P321$) have been investigated by powder diffraction. Considering the difficulties in discriminating between the $KAl(SO_4)_2$ and the new $CsV(SO_4)_2$ structure type, it is possible that some of these structures crystallize in $P\bar{3}$ as well. It may be worthwhile to reinvestigate some of these compounds by single crystal diffractometry.

Table II gives the coordinates of the atoms at 140 K and the isotropic thermal parameters, respectively. Figure 2 shows a stereopair of the $CsV(SO_4)_2$ structure, from which the coordination spheres of Cs, V and S can be visualized. The important interatomic distances and bond angles of the structure are collected in Table III. A table of anisotropic temperature parameters is included as supplementary material.

Discussion of the Crystal Structure

The crystal structure consists of a unique arrangement of tetrahedral SO_4^{2-} anions linked to octahedrally coordinated vanadium(III) and to Cs^+ ions in a 6 + 6 oxygen coordination formed by two interpenetrating trigonal antiprisms of O(1) and O(2) atoms.

The VO_6 octahedra are corner-connected to the SO_4^{2-} tetrahedra and form a triple polymeric layer of composition $[V(SO_4)^-_2]_n$, separated by layers of Cs^+ ions. Both layers are parallel to (001). The VO_6 octahedron is not far from being regular with all bonds equally long and O(2)–V–O(2) angles of 88.8 and 91.2° (±0.1°) in the slightly elongated $\bar{3}$ octahedron. Within the SO_4^{2-} ion, the S–O(1) bond length is significantly

(12) Strupler, N.; Morette, A.; Peutat, L. *Bull. Soc. Chim. Fr.* **1970**, 1671.
(13) Strupler, N. *Bull. Soc. Chim. Fr.* **1970**, 2451.
(14) Larson, A. C. *Crystallographic Computing*, Munksgaard, Copenhagen, 1970, p 291.
(15) *International Tables for X-Ray Crystallography*, Kynoch Press: Birmingham, England, 1968; Vol. III.
(16) Cruickshank, D. W. J. *Crystallographic Computing*; Munksgaard: Copenhagen, 1970, p 187.
(17) Vegard, L.; Maurstad, A. *Z. Kristallogr.* **1929**, *69*, 519.
(18) Franke, W.; Hennig, G. *Acta Crystallogr.* **1965**, *19*, 870.
(19) Manoli, J.-M.; Herpin, P.; Pannetier, G. *Bull. Soc. Chim. Fr.* **1970**, 98.
(20) Hutton, C. O. *Am. Mineral.* **1959**, *44*, 1105.
(21) Graeber, E. J.; Rosenzweig, A. *Am. Mineral.* **1971**, *56*, 1917.
(22) Anthony, J. W.; McLean, W. J.; Laughon, R. B. *Am. Mineral.* **1972**, *57*, 1546.
(23) Perret, R.; Couchot, P. *C. R. Seances Acad. Sci., Ser C* **1972**, *274*, 55.
(24) Pannetier, G.; Manoli, J.-M.; Herpin, P. *Bull. Soc. Chim. Fr.* **1972**, 485.
(25) Chizov, S. M.; Pokrovskii, A. N.; Kovba, L. M. *Kristallografija* **1982**, *27*, 997.
(26) Sirotinkine, S. P.; Tchijov, S. M.; Pokrovskii, A. N.; Kovba, L. M. *J. Less-Common Met.* **1978**, *58*, 101.
(27) Sirotinkin, S. P.; Efremov, V. A.; Kovba, L. M.; Pokrovskii, A. N. *Kristallografija* **1978**, *23*, 406.
(28) Degtyarev, P. A.; Pokrovskii, A. N.; Kovba, L. M. *Kristallografija* **1978**, *23*, 840.
(29) Bukovec, N.; Golic, L.; Bukovec, P.; Siftar, J. *Monatsh. Chem.* **1978**, *109*, 1305.
(30) Bukovec, N.; Kaucic, V.; Golic, L. *Acta Crystallogr.* **1980**, *B36*, 129.
(31) Sirotinkin, S. P.; Pokrovskii, A. N.; Kovba, L. M. *Kristallografija* **1981**, *26*, 385.

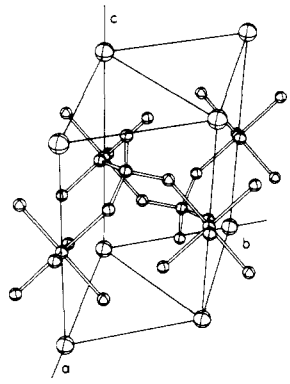

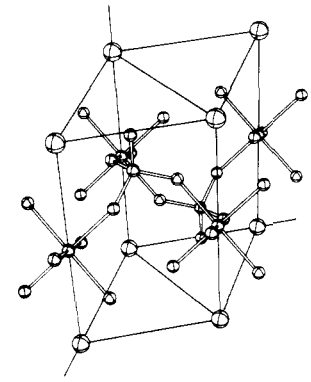

Figure 2. Stereo pair of the $CsV(SO_4)_2$ structure.

Table III. Interatomic Distances (Å) and angles (deg) in $CsV(SO_4)_2$ (with Standard Deviations)

Cs–O(1)	3.079(1) (6×)	S–O(2)	1.484(1) (3×)
Cs–O(2)	3.591(2) (6×)	V–O(2)	1.995(1) (6×)
S–O(1)	1.448(2)		
O(2)–V–O(2)	88.8(1), 91.2(1), 180.0(1)	O(2)–S–O(2)	109.1(1) (3×)
O(2)–S–O(1)	109.8(1) (3×)		
Cs···V	4.384(1)	Cs···S	3.901(1)
Cs···Cs	4.868(1)		

shorter than the S–O(2) bond length. This may be due to the stronger interaction of the triply coordinated O(2) with vanadium as compared to the weaker interaction of the tetrahedrally coordinated O(1) with cesium. Analogous distortions of SO_4^{2-} tetrahedra were observed in $NaV(SO_4)_2$[7] and $KV(SO_4)_2$.[5] Table IV shows the interatomic distances of oxygen in $CsV(SO_4)_2$, and $KV(SO_4)_2$ and $NaV(SO_4)_2$.

The observed crystal structure of $CsV(SO_4)_2$ is unique: Apparently, there is no other example of this structure type known in the structural chemistry of double sulfates or of other non-sulfate double salts of this stoichiometry as well.

In Table V, some features of the by now known structure prototypes are listed. There is a remarkably close relationship between the new $CsV(SO_4)_2$ structure and the four structure types $KAl(SO_4)_2$, $KFe(SO_4)_2$, $RbTl(SO_4)_2$, and $KV(SO_4)_2$. All five structures contain very similar triple sheets of composition $[M^{III}(SO_4)_2^-]_n$ with M^{III} = Al, Fe, V or Tl, alternating with layers of alkali-metal ions. The thickness of such a cation–anion layer package is around 8 Å. The difference between the members of this structural family consists of a different coordination of the metal centers, especially the M^{III} metals. The shapes of the unit cells of $RbTl(SO_4)_2$ and $KV(SO_4)_2$ and of $KAl(SO_4)_2$ and $CsV(SO_4)_2$ are very similar. In both cases the only difference is the position of O(2), changing the coordination of M^{III} from trigonal-prismatic thallium(III) and aluminum(III) to octahedral vanadium(III).

Spectroscopic Investigations

General Considerations. A standard analysis of the crystal selection rules for infrared and Raman spectra, based on group theoretical principles[32-34] is summarized in Table VI. The polarization properties of the Raman activity in Table VI are determined under the assumption that the electronic ground state is totally symmetric. Powder results by Strupler[13] and single-crystal results by us show that the room temperature and low temperature structures are the same. In total, 10 Raman fundamentals ($5A_g + 5E_g$) and 12 IR fundamentals ($6A_u + 6E_u$) should be spectroscopically observable by letting suitably polarized light interact with powders or oriented crystals.

Table IV. Coordination Spheres of Oxygen in $CsV(SO_4)_2$, $KV(SO_4)_2$, and $NaV(SO_4)_2$ and Bond Lengths (Å) (with Standard Deviations)

coordination	$CsV(SO_4)_2$[a]		$KV(SO_4)_2$[b]		$NaV(SO_4)_2$[c]	
oxygen not coordinated to vanadium	O–S	1.448(2)	O–S	1.455(5)	O–S	1.433(2)
	O–Cs	3.079(1)	O–K	2.867(1)	O–Na	2.439(2)
oxygen coordinated to vanadium	O–S	1.484(1)	O–S	1.496(5)	O(1)–S	1.475(2)
					O(3)–S	1.490(1)
	O–Cs	3.591(2)	O–K	3.275(1)	O–Na	2.534(1)
	O–V	1.995(1)	O–V	1.996(4)	O(1)–V	1.962(2)
					O(3)–V	2.016(1)

[a] This work. [b] Reference 5. [c] Reference 7.

The internal vibrations of a regular tetrahedral SO_4^{2-} ion (T_d point group) span the representation

$$\Gamma_{vib} = A_1(\nu_1) + E(\nu_2) + 2F_2(\nu_3 + \nu_4)$$

of which all are Raman and F_2 is IR permitted. Modes labeled ν_1 and ν_3 are stretchings, and ν_2 and ν_4 are bendings, in the usual approximation of weak couplings.

In $CsV(SO_4)_2$, the two SO_4^{2-} ions present in the unit cell have 18 internal degrees of vibrational freedom, which should be distributed on the symmetry species and original sulfate modes ν_1–ν_4 as shown in Table VII.

The frequencies of the fundamentals of the SO_4^{2-} ion have been well characterized,[35,36] mainly by Raman spectroscopy on aqueous solutions: $\nu_1(A_1) \simeq 981\ cm^{-1}$, $\nu_2(E) \simeq 451\ cm^{-1}$, $\nu_3(F_2) \simeq 1104\ cm^{-1}$, and $\nu_4(F_2) \simeq 613\ cm^{-1}$. Within the crystal, sulfate frequency shifts are expected similar to what was found for $KV(SO_4)_2$.[5]

Infrared Spectra. The IR-spectrum of $CsV(SO_4)_2$ at room temperature is shown in Figure 3. The IR-bands can easily and unambigously be assigned according to the selection rules as shown in Table VIII. The assignments are completely analogous to the $KV(SO_4)_2$ case.[5]

Raman Spectra. Raman spectra (see Figures 4–7) were measured at room and liquid nitrogen temperatures (actual temperature 100–106 K) on oriented single crystals and on polycrystalline samples (not shown). For excitation, horizontal argon ion laser beams of wavelength 514.5, 488.0, or 476.5 nm and of vertical polarization were used. The scattered light was collected at an angle of 90°, analyzed with a Polaroid-sheet polarizer, and sent through a 90° image rotator and a polarization scrambler; the entrance slit was vertical and the scattering plane

(32) Fateley, W. G.; McDevitt, N. T.; Bentley, F. F. *Appl. Spectrosc.* **1971**, *25*, 155.
(33) Adams, D. M. *Coord. Chem. Rev.* **1973**, *10*, 183. Adams, D. M.; Newton, D. C. *Tables for Factor Group and Point Group Analysis*; Beckman-RIIC Ltd.: Croydon, England, 1970.
(34) Rousseau, D. L.; Bauman, R. P.; Porto, S. P. S. *J. Raman Spectrosc.* **1981**, *10*, 253.
(35) Siebert, H. *Applications of Vibrational Spectroscopy in Inorganic Chemistry*; Springer-Verlag: Berlin, 1966.
(36) Nakamoto, K. *Infrared and Raman Spectra of Inorganic and Coordination Compounds*; Wiley: New York, 1978; p 142.

Table V. Structural Features of Double-Sulfate Types

$M^IM^{III}(SO_4)_2$	space group	coordination M^I	coordination M^{III}	quotient of ionic radii[a] M^{III}/M^I	refs
$KAl(SO_4)_2$	$P321$	6 + 6	6 (trigonal prismatic)	0.38	17–19
$KFe(SO_4)_2$	$C2/m$	10	6 (octahedral)	0.41	20–23
$NaV(SO_4)_2$	$C2/m$	8	6 (octahedral)	0.60	7
$KV(SO_4)_2$	$R\bar{3}$	6 + 6	6 (octahedral)	0.45	5
$CsV(SO_4)_2$	$P\bar{3}$	6 + 6	6 (octahedral)	0.39	this work
$RbTl(SO_4)_2$	$R32$	6 + 6	6 (trigonal prismatic)	0.55	24
α-$NaTm(SO_4)_2$	$P2_1/m$	8	8 (polyhedral)	0.87	25
$NaEr(SO_4)_2$	$P2_1/b$	8	8 (polyhedral)	0.88	26
$NaNd(SO_4)_2$	$P\bar{1}$	8	9 (polyhedral)	0.97	26
$LiPr(SO_4)_2$	$P2_1/b$	4	9 (polyhedral)	1.77	27
$KPr(SO_4)_2$	$P\bar{1}$	12	8 (polyhedral)	0.74	28
$CsPr(SO_4)_2$	$Pnna$	14	8 (polyhedral)	0.63	29
$CsLa(SO_4)_2$	$P2_1/n$	13	9 (polyhedral)	0.66	30
$LiLu(SO_4)_2$	$Pbcn$	6 + 4	6 (octahedral)	1.12	31

[a] Calculated by use of "crystal ionic radii": Shannon, R. D., Prewitt, C. T. *Acta Crystallogr.* **1969**, *B25*, 925; **1970**, *B26*, 1046.

Table VI. Analysis of the Selection Rules for $CsV(SO_4)_2$, Space group S_6^1 ($P\bar{3}$, No. 147)[a]

S_6 point group	T_A	T	R	N_I	Raman activity	IR activity
A_g		1	1	3 (ν_1, ν_3, ν_4)	x^2+y^2, z^2	
E_g		1	1	3 (ν_2, ν_3, ν_4)	(x^2-y^2, xy) (xz, yz)	
A_u	1	2	1	3 (ν_1, ν_3, ν_4)		z
E_u	1	2	1	3 (ν_2, ν_3, ν_4)		x, y

[a] The Bravais primitive cell contains one formula with Cs on Wyckoff site 1*a* (S_6 symmetry), V on site 1*b* (S_6 symmetry), S and O(1) on site 2*d* (C_3 symmetry), and O(2) on site 6*g* (C_1 symmetry). T_A = inactive acoustic modes, T = optic-branch translatory modes, R = rotatory modes (of SO_4^{2-}), and N_I = internal modes (of SO_4^{2-}).

horizontal. Essentially identical spectra were obtained regardless of wavelength. In Figures 4–7, the polarization of the exciting and scattered light was varied using a $\lambda/2$ plate and the polarizer, respectively, as indicated by the standard label $x(yz)q$. In terms of crystallographic directions, the label $x(yz)q$ describes the experiment; x = excitation beam propagation direction, y = excitation beam polarization direction, z = collection polarization direction, and q = collection direction. In our case of a trigonal crystal, an auxiliary direction b', defined by $a \times c$, was used.

Ten Raman bands (six internal SO_4^{2-} vibrations, two SO_4^{2-} rotations, and two translations) are expected (Tables VI and VII) in the crystal spectra ($5A_g$ and $5E_g$). The centrosymmetry of the crystal excludes the bands from being seen in both IR and Raman (gerade–ungerade classification). From Figures 4–7 and Table VIII it can be seen that 11 (at low temperatures), instead of 10, bands are present in the Raman spectra below 1300 cm^{-1}. Furthermore, the crystal spectra show significant polarization abnormalities. From Table VI it is expected that all Raman bands originating from a vibrational state of E_g symmetry should be absent in the (cc) polarization, while bands due to vibrational states of A_g symmetry should be absent in the off-diagonal polarizations (ac), etc. Thus, the (cc) and (ac) spectra of Figures 4–7 should have no bands in common. It is obvious that this is not the case. The deviations from the expected polarization behavior is far too great to be due to so-called "leakage", that is imperfect polarization due to beam convergence and optical imperfection.

It should be noted that the orientation of the single crystals was definitely correct due to the easily recognized direction of the *c* axis which was perpendicular to the flat side of the crystal. Also, several crystals gave identical spectra, some of them obtained in another laboratory.[37]

It is very astonishing that there is not a clearly polarized ν_1-(A_g) sulfate stretching band present in the spectrum. From previous spectroscopic experiences[5,35,36] it is evident that the ν_1-(A_g) mode of $CsV(SO_4)_2$ ought to be intense and in the frequency range 900–1000 cm^{-1}. Thus, the strong doublet band at ~900 cm^{-1} is assigned to A_g. Other bands below 1300 cm^{-1} are tentatively assigned to symmetry as given in Table VIII.

The broad weak bands above ~1300 cm^{-1} are attributed to electronic Raman transitions of the V^{3+} ion. A characteristic feature of electronic Raman bands is that they are generally much broader than vibrational bands, even at very low temperatures.[38,39]

As discussed in the report on $KV(SO_4)_2$[5], the ground electronic state of $V^{3+}(d^2)$ in an octahedral crystal field is $^3T_{1g}(^3F)$, which in the trigonal S_6 field splits into a ^3E_g state and a ^3A_g state.[40,41] It is normally assumed that the ^3A_g state is the ground state. Similar splittings occur in the two excited triplet states $^3T_{2g}(^3F)$ and $^3T_{1g}(^3P)$. In Figure 8, we have estimated the electronic states of V^{3+} in octahedral oxide fields using a theoretical energy diagram[41] with the $Dq \simeq 1500$ cm^{-1}. On the same figure the absorption spectrum[5] of solid $KV(SO_4)_2$ is also presented. The observed bands in the visible region are attributed to V^{3+} transitions in the S_6 crystal field:

$$^3A_g(^3F, ^3T_{2g}) \leftarrow {}^3A_g(^3F, ^3T_{1g}),\ \nu_a \approx 13400\ cm^{-1}$$

$$^3E_g(^3F, ^3T_{2g}) \leftarrow {}^3A_g(^3F, ^3T_{1g}),\ \nu_b \approx 14600\ cm^{-1}$$

These values are obtained by resolving the broad feature centered at ~14 400 cm^{-1} into Gaussians. The deconvolution is made by assuming that the relative intensities of the two bands is the same as in the case of $KV(SO_4)_2$. The shoulder band in the near UV region is assigned to the split component, ^3A_g, of the second triplet excited state $^3T_{1g}(^3P)$:

$$^3A_g(^3P, ^3T_{1g}) \leftarrow {}^3A_g(^3F, ^3T_{1g}),\ \nu_c \approx 22\,500\ cm^{-1}$$

The separation of the $^3A_g(^3T_{2g})$ and $^3E_g(^3T_{2g})$ states is $\Delta\nu = \nu_b - \nu_a \approx 1200$ cm^{-1}, which according to ligand field calculations[40,41] is smaller than the separation of the $^3E_g(^3T_{1g})$ and $^3A_g(^3T_{1g})$ in the ground state. In other words, for the V^{3+} ion in a $\bar{3}$ crystal, the first electronic Raman transition is likely to occur in a region

(37) Clark, R. J. H. Private communication.

(38) Koningstein, J. A. *Ionic and Molecular Electronic Raman Spectroscopy.* Chapter 5 in *Mol. Spectrosc.* **1976**, *4*, 196. Koningstein, J. A. On the Relevance of the Vibro-Electronic and Electronic Raman Effect. Chapter 2 in *Vib. Spectra Struct.* **1981**, *9*, 115.
(39) Clark, R. J. H.; Dines, T. J. Electronic Raman Spectroscopy. Chapter 5 in *Adv. Infrared Raman Spectrosc.* **1982**, *9*, 282.
(40) Hush, N. S.; Hobbs, R. J. M. Absorption Spectra of Crystal Containing Transition Metal Ions. *Prog. Inorg. Chem.* **1968**, *10*, 259.
(41) Ferguson, J. Spectroscopy of 3d Complexes. *Prog. Inorg. Chem.* **1970**, *12*, 159.
(42) Macfarlane, R. M. *J. Chem. Phys.* **1964**, *40*, 373.

Table VII. Correlation Diagram for SO_4^{2-} Internal Vitrations[a]

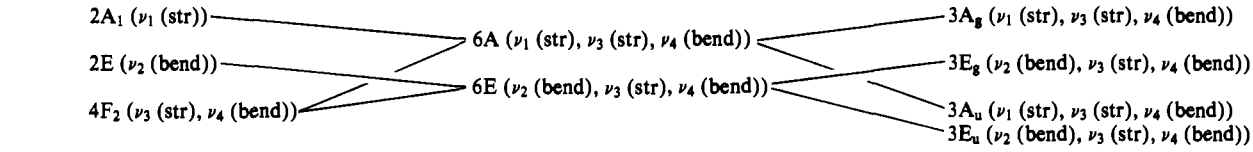

[a] The site symmetry is C_3 and the unit cell symmetry is C_6^1, with the 3 and $\bar{3}$ axes fixed to the crystallographic *c*-axis.

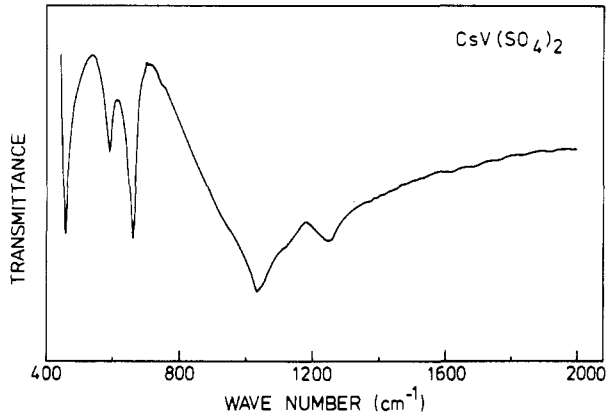

Figure 3. Infrared spectrum of $CsV(SO_4)_2$ powder in CsBr disk at room temperature.

Table VIII. Infrared and Raman Bands (cm^{-1}) of $CsV(SO_4)_2$ and Assignments[a]

IR powder (Figure 3)	Raman cryst (Figure 4)	tentative assignt	SO_4^{2-} vibr freq[b]
	~1400 w	ν_c ($^3E_g \rightleftharpoons {}^3A_g$)[c]	
	1279 m	ν_3	
1258 s		ν_3	
			1105 (ν_3)
	1050 s	ν_3	
1033 vs		ν_3	
944 vw		ν_1 (A_u)	
			983 (ν_1)
	924 s[d,e]		
	896 s[d]	ν_1 (A_g)	
662 vs		ν_4	
			611 (ν_4)
	645 m	ν_4	
	597 w	ν_4	
593 s		ν_4	
	467 s	ν_2 (E_g)	
458 vs		ν_2 (E_u)	450 (ν_2)
	308 s	ν_L[f]	
	227 w	ν_L	
	175 s	ν_L	
	115 m	ν_L	

[a] Intensity codes: w = weak, m = medium, s = strong, v = very. [b] Aqueous solution: ref 37. [c] ν_c: electronic mode (see text). [d] Values obtained by resolving bands at liquid nitrogen temperature. [e] Presumably overtone or combination. [f] ν_L: external lattice mode.

near 1400 cm^{-1}. The broad structured Raman band above ~1300 cm^{-1} is in this expected range and is thus assigned to the $^3E_g(^3T_{1g}) \leftarrow {}^3A_g(^3T_{1g})$ electronic transition. Such a transition is permitted according to the electronic Raman selection rules since the direct product $A_g \otimes E_g$ includes the representation E_g, which belongs to the Raman polarizability tensor components.[38,39]

Based on crystal-field model calculations, the splitting of octahedral states in trigonal fields of intermediate strength can be calculated in terms of two parameters v and v'.[40-42] For the triplet states in Figure 8 the splittings are

The values of the first two splittings measured from the spectra, are ~1400 and ~1200 cm^{-1}, respectively, and thus v = ca. 2400 and v' = ca. −1500 cm^{-1}. From the third difference, the energy

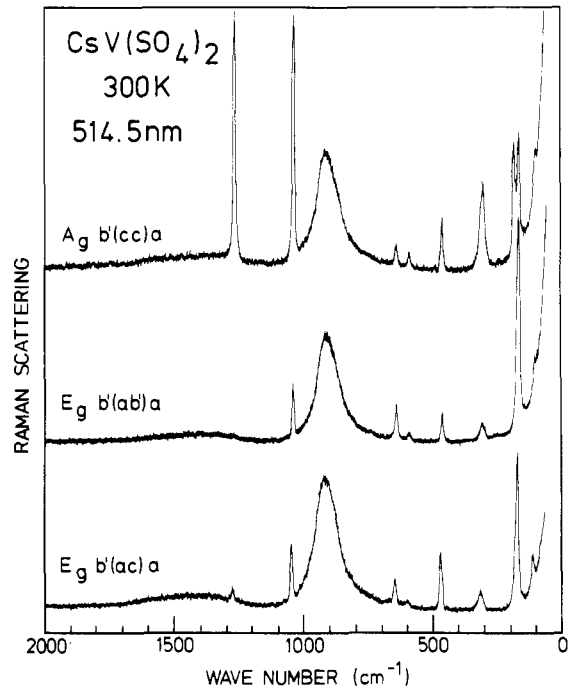

Figure 4. Raman spectra of a $CsV(SO_4)_2$ crystal at room temperature, under three different orientation/polarization setups and with an excitation wavelength of 514.5 nm.

of the upper $^3E_g(^3P, {}^3T_{1g})$ state can be estimated to ca. 24 500 cm^{-1}, based on ν_c = ca. 22 500 cm^{-1}.

As remarked above, the crystal Raman spectra show anomalous polarization properties. Also, the band at ca. 900 cm^{-1} is surprisingly broad and splits into two bands at lower temperatures. The band is without question real and a corresponding band was seen[5] for $KV(SO_4)_2$. As presented below, the anomalous polarization can be attributed to possible interactions between the vibrational and electronic states in the crystal. As shown in Figure 8, where the estimated electronic states of $V^{3+}(3d^2)$ in the S_6 field are illustrated, the green to blue laser lines used in order to excite the Raman spectra overlap strongly with the tail of the Laporte-forbidden UV absorption bands, corresponding to transitions from the ground state to the $^3A_g(^3P,{}^3T_{1g})$ and $^3E_g(^3P,{}^3T_{1g})$ levels. Therefore the electronic and vibrational Raman bands might exhibit preresonance enhancement of their intensities[39] and a series of combinations and/or overtones of fundamental vibrations might be observed in the Raman spectrum.

Consequently, one of the bands contributing to the broad/double feature at ~900 cm^{-1} can be due to a combination or an overtone of fundamentals whose intensity enchancement could be accounted for by the pre-resonance conditions described or by the possibility of a Fermi resonance with the $\nu_1(A_g)$ mode (e.g. the first overtone of $\nu_2(E_g)$ could result in a state derived from the cross product $E_g \otimes E_g$ which contains the symmetry species A_g and E_g). A Fermi resonance would account also for the strong temperature dependence of the relative intensities of the two bands. It seems less likely that one of the bands could be of electronic origin, the other being the ν_1 vibrational band. Electronic transitions are generally weak and broad, even at ~100 K, and

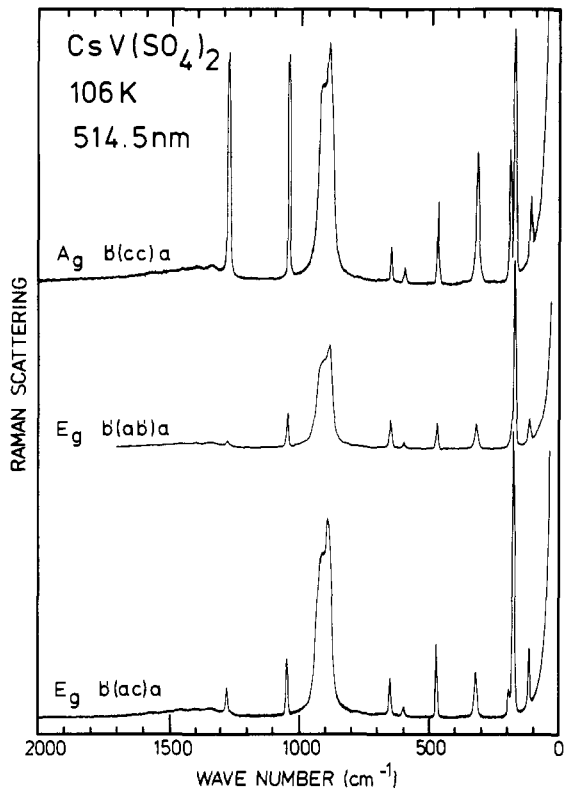

Figure 5. Raman spectra of a $CsV(SO_4)_2$ crystal at low temperature (106 K), under three different orientation/polarization setups and with an excitation wavelength of 514.5 nm.

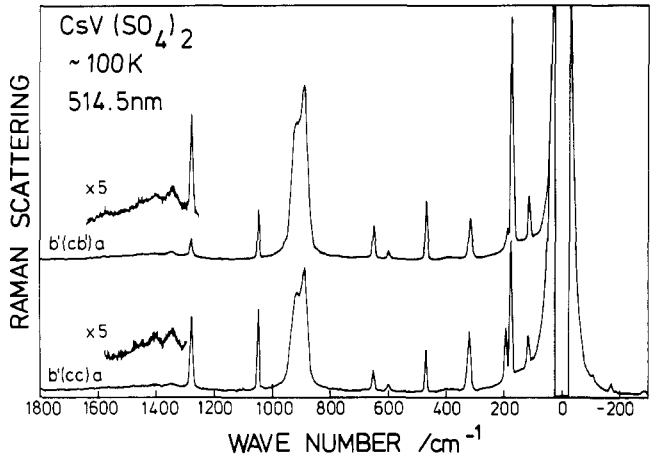

Figure 6. Raman spectra of a $CsV(SO_4)_2$ crystal at low temperature (~100 K), under two different orientation/polarization setups and with an excitation wavelength of 514.5 nm. Anti-Stokes lines are included, and the region ~1300 to ~1600 cm^{-1} is shown magnified.

it is not expected that a resonance between a totally symmetric vibrational state and an electronic state can transfer appreciable intensity from the vibrational to the electronic band.

Furthermore, the ground electronic state is spin-degenerate and as it has been pointed out previously[39,43,44] this may induce spin–orbit interactions that may cause mixing of the spin and orbital functions, resulting in a degenerate ground state.

As previously noted, the expected polarization properties are derived under the assumption of a totally symmetric electronic ground state. The situation is different if the electronic state is degenerate, as in this case of E_g symmetry. The magnitudes of depolarization ratios for totally symmetric vibrations (i.e. such

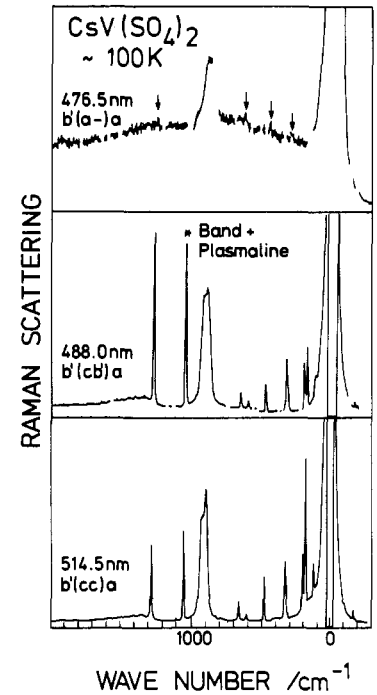

Figure 7. Raman spectra of a $CsV(SO_4)_2$ crystal at low temperature (~100K), under different orientation/polarization setups and with different excitation wavelengths. Regions where plasma lines could not be filtered are omitted for the 476.5 nm spectrum.

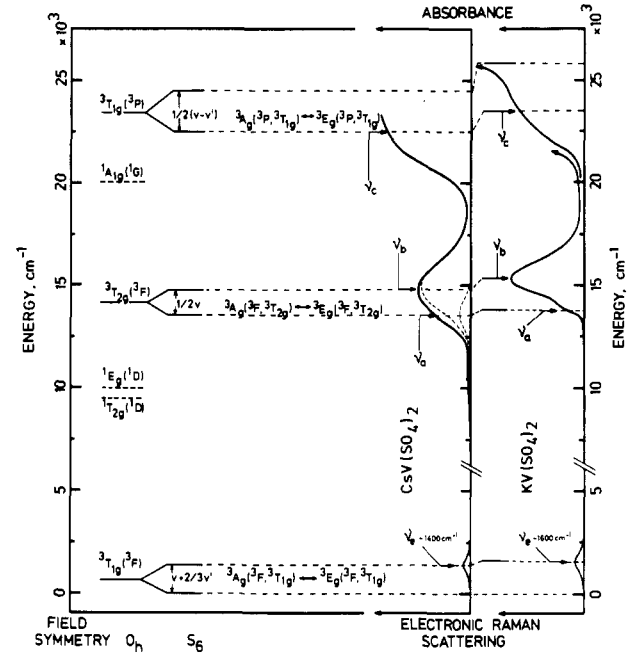

Figure 8. Energy states of V^{3+} with Dq = ca. 1500 cm^{-1} in an octahedral O_h field and splittings of triplet states in the trigonal S_6 field of the $CsV(SO_4)_2$ crystal. O_h energy states underlined by broken lines indicate states associated with spin-forbidden transitions from the ground state. The absorption ($\nu_a - \nu_c$) and electronic Raman (ν_e) bands of crystalline $CsV(SO_4)_2$ are shown in arbitrary intensity units. To the right, the respective spectra of crystalline $KV(SO_4)_2$[5] are included for comparison. It is not certain which of the S_6 states, ^3A_g or ^3E_g, is the ground state.

as the $\nu_1(A_g)$) in systems with a degenerate ground state are expected to be significantly altered. The symmetry species for such vibrational transitions will contain also irreducible representations other than the totally symmetric one, thus gaining some antisymmetric character. This results in anomalous depolarization ratios for the totally symmetric vibrational Raman band.[39] In other words, in such a case the selection rules predicted by standard group-theoretical analysis are broken. Then, using

(43) Hamaguchi, H. *J. Chem. Phys.* **1978**, *69*, 569.
(44) Clark, R. J. H. and Turtle, P. C. *J. Chem. Soc., Faraday Trans.* **1976**, *2*, *72*, 1885.

$$\Delta[^3T_{1g}(^3F)] = v + {}^2/_3\, v'$$

$$\Delta[^3T_{2g}(^3F)] = {}^1/_2\, v$$

$$\Delta[^3T_{1g}(^3P)] = {}^1/_2(v - v')$$

the methods for deriving the possible nonvanishing tensor components given elsewhere,[45] we find that vibrational modes of E_g symmetry will indeed show activity in the cc polarization and modes of A_g symmetry will be active in ac polarization. Therefore one explanation for the anomalous polarization properties could be a ^3E_g electronic ground state.

The explanations given above are tentative and must be checked against further experimental and theoretical results which are in progress.

(45) Mortensen, O. S.; Hassing, S. *Adv. Infrared Raman Spectrosc.* **1979**, *6*, 1.

Conclusion. Examination of the compound $CsV(SO_4)_2$ has been performed: It has a unique structure in space group $P\bar{3}$ which allows for the interpretation of the IR spectrum and, by incorporating the electronic Raman effect and "anomalous" depolarization effects, also the Raman spectrum.

Acknowledgment. This investigation has been supported by the Science program of the European Economic Community (EEC Contract No. SC1*/0181-C(AM) and by The Danish Natural Science Research Council. Kim Michael Eriksen of The Technical University of Denmark is thanked for experimental assistance. Financial support by the Fonds der Chemischen Industrie is gratefully acknowledged.

Supplementary Material Available: A table of anisotropic temperature parameters (Table A) (1 page). Ordering information is given on any current masthead page.